

Growth of Embedded and Protrusive Striped Graphene on 6H-SiC (0001)

A. Ruammitree*, H. Nakahara, K. Soda, Y. Saito

Department of Quantum Engineering, Faculty of Engineering, Nagoya University, Nagoya
464-8603 Japan

Abstract: We have studied the growth of the epitaxial graphene by annealing Si-terminated SiC (0001) under Ar pressure of 0.05 atm and 0.3 atm. In the case of annealing SiC substrate under Ar pressure of 0.05 atm, graphene prefers to be grown and embedded at step edge. For annealing SiC substrate under Ar pressure of 0.3 atm, free C and Si atoms, which released from the SiC decomposition, diffuse to the step edge and nucleate protrusive graphene. Raman peak characteristics reveal the embedded and protrusive graphene has approximately the same carrier concentration and strain.

Index Terms— graphene, SiC, carbon diffusion, reflection high-energy electron diffraction, scanning electron microscope, atomic force microscopy, Raman spectroscopy, angle-resolved photoemission spectroscopy

I. INTRODUCTION

Graphene is a two dimensional carbon material which its carbon atoms are packed in a honeycomb crystal lattice. Graphene has many exotic properties such as high mobility and linear dispersion (Dirac cone) at the K-point in the Brillouin zone [1], [2]. Graphene can be fabricated by many methods such as mechanical exfoliation of graphite, chemical vapor deposition (CVD) of carbon-bearing gases on the surface of copper films [3], [4], opening carbon nanotubes [5] and annealing SiC substrate. Graphene nanribbons (GNRs) are strips of graphene with narrow width. The electronic property of GNRs depends on the width and edge structure. GNRs can be fabricated by cutting down larger graphene (such as e-beam lithography) [6] and bottom-up growth. Annealing SiC substrate is one of suitable methods for fabricating bottom up GNRs with intact edge. GNRs on SiC can be applied for many application such as field-effect transistors [7]. In this study, we have demonstrated the growth of GNRs on Si-terminated 6H-SiC (0001) by annealing the SiC substrates under Ar atmosphere.

II. EXPERIMENTAL

N-type Si-terminated 6H-SiC (0001) substrates were employed and first cleaned by ultrasonic precleaning with acetone. After that the substrates were put in a main chamber with the base pressure of $\sim 10^{-10}$ mbar and deposited by Si atoms around 2 layers. Then the substrates were transferred, without exposure to air, to another annealing chamber before annealed them by resistive heating under an Ar gas pressure of 0.05 and 0.3 atm. The annealing temperature was in range of ~ 900 to graphitization temperature (1550 °C and 1675 °C)

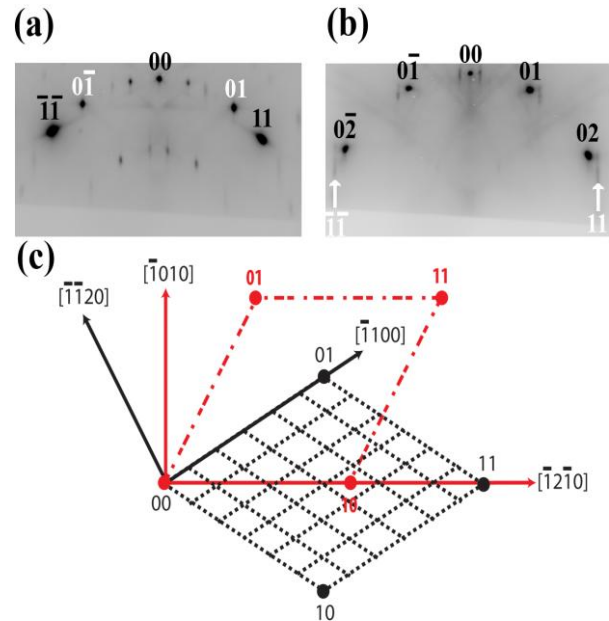


Fig 1. the RHEED pattern shows 6×6 reconstruction of 0.05 atm sample after annealed at graphitization temperature (1550 °C) and the beam direction of $[1010]$ (a) and $[1120]$ (b). White and black number indicate the positions of reflections from graphene and SiC substrate, respectively. (c) schematic of reciprocal lattices of 6×6 reconstruction. Red and black circles represent reflections from 1×1 graphene and SiC surface reconstruction, respectively.

with steps of $\sim 100^\circ\text{C}$ (10~15 min per each step). The annealing temperature was measured by an optical pyrometer.

After annealing, Reflection high-energy electron diffraction (RHEED) which has incident beam energy of 10 kV was employed to measure the structure of SiC surface in the main chamber (base pressure of $\sim 10^{-10}$ mbar). The RHEED patterns were recorded by a CCD camera. The topography of samples was measured by atomic force microscopy (AFM) in air. An Ultra-high vacuum scanning electron microscope (UHV-SEM) which has incident beam of 2.2 KeV was performed to confirm the shape and position of graphene. Raman spectroscopy was used with wavelength at 532 nm. Angle-resolved photoemission spectroscopy (ARPES) measurement was conducted at room temperature at the beam line 5U of UVSOR-II in the Institute for Molecular Science, Okazaki, Japan. The excitation photon energy was set to 80 eV.

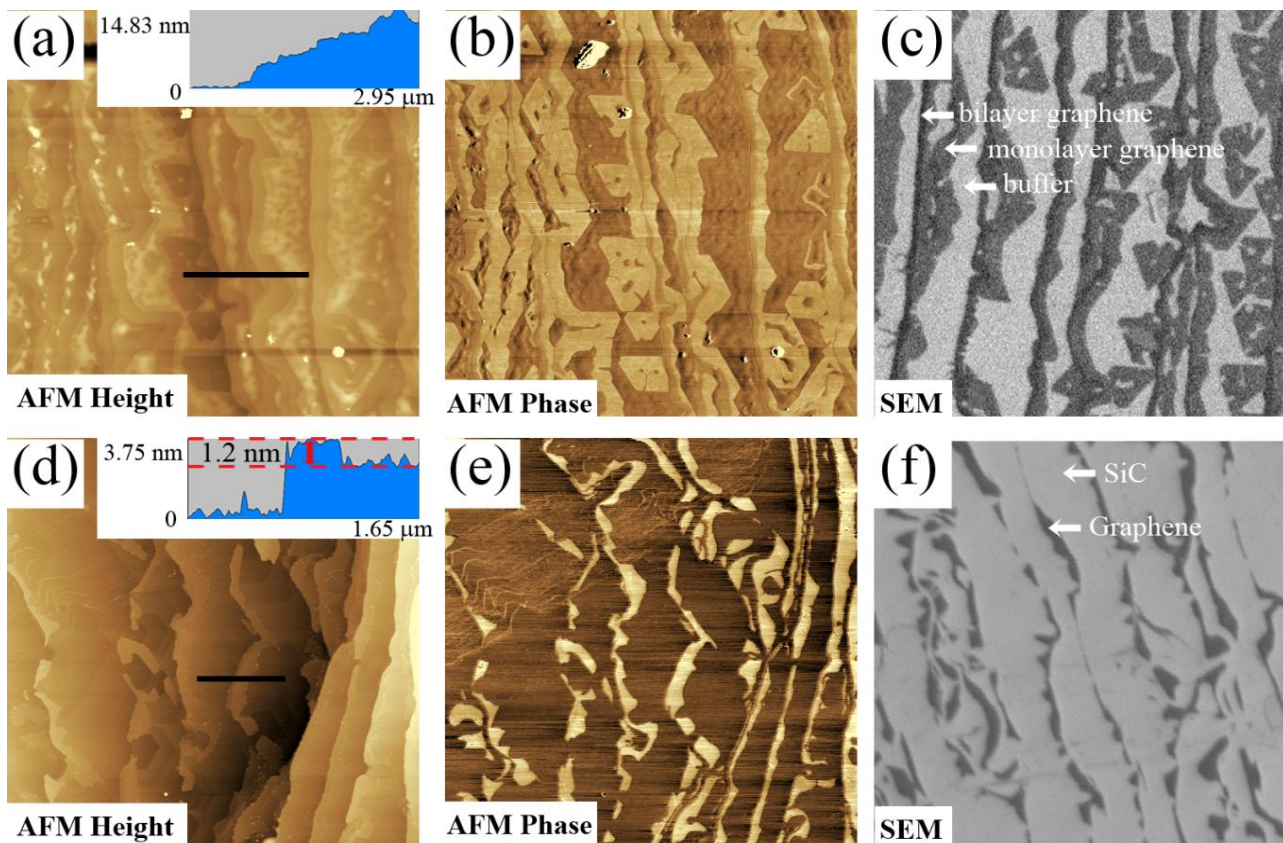


Fig 2 AFM (a, b and d, e) and SEM (c and f) images of 0.05 atm (a-c) and 0.3 atm (d-f) samples. (a) and (d) inset Line profiles along black lines. Bright regions in AFM phase image (b and e) and black regions in SEM image (c and f) indicate graphene regions.

III. RESULTS AND DISCUSSION

After annealing, the samples were transferred to measure the evolution of the surface structure by RHEED. The results show that in the case of the sample which annealed under Ar pressure of 0.05 atm (0.05 atm sample) the structure evolves from $1 \times 1 \rightarrow \sqrt{3} \times \sqrt{3} \rightarrow 6 \times 6$ reconstruction at annealing temperature of 1350 °C and 1550 °C, respectively. In the case of annealing the sample under Ar pressure of 0.3 atm (0.3 atm sample), the structure changes from $1 \times 1 \rightarrow 3 \times 3 \rightarrow 6 \times 6$ reconstruction after annealing at the temperature of 1300 °C and 1675 °C. Annealing under Ar pressure of 0.3 atm can shift the graphitization temperature due to the reduction of Si sublimation. Namely, the presence of higher pressure of Ar gas increase probability of Si collision with Ar atoms leads to number of reflected Si atoms back to the surface increases. Fig 1 (a) and (b) show the surface structure of 6×6 reconstruction measured by RHEED after annealed at the graphitization temperature (1550 °C) under Ar pressure of 0.05 atm. The reflections from graphene are appeared around $(0.72, 0.72)$ and $(\overline{0.72}, \overline{0.72})$ positions when the incident beam was applied in the $[\overline{1}010]$ direction [8]. In addition, when the sample was rotated by 30 degree ($[\overline{1}\overline{1}20]$ incidence), the reflections from graphene are observed near $(0, \pm 2)$ positions (indicated by arrows). Fig 1 (c) shows a

schematic of the reciprocal lattice of 6×6 reconstruction where a red dash line rhombohedron represents a graphene unit cell which has the different angle of 30 degree from a SiC unit cell (black dot line).

In this study, we annealed the SiC substrates by resistive heating method. This method can give us a non-uniform temperature on the SiC substrates leads to the non-uniform graphene thickness on the sample. This method also gives us opportunities for measuring the graphene morphology and shape from their initial state. Fig 2 shows AFM and SEM images of the 0.05 atm (Fig 2 (a)-(c)) and 0.3 atm samples (Fig 2 (d)-(f)). In the case of 0.05 atm sample, Fig 2 (a) and (b) are AFM topographic and phase images (respectively) showing the position of graphene regions (bright regions in Fig 2 (b)) on this sample is lower than that of their terrace as shown clearly by the line profiles (Fig 2 (a) inset) along the black line. We also found that the graphene is first nucleated at upper step edge with the position lower than its bare SiC terrace. It is attributed to the SiC decomposition which prefers to occur at step edge due to the instability. SEM image (Fig 2 (c)) shows 3 distinctive SEM contrasts i.e. bright, dark gray and black (narrow striped line) indicating buffer layer, monolayer and bilayer graphene, respectively.[9] SEM results confirm the bright region in AFM phase image (Fig 2 (b)) is graphene regions.

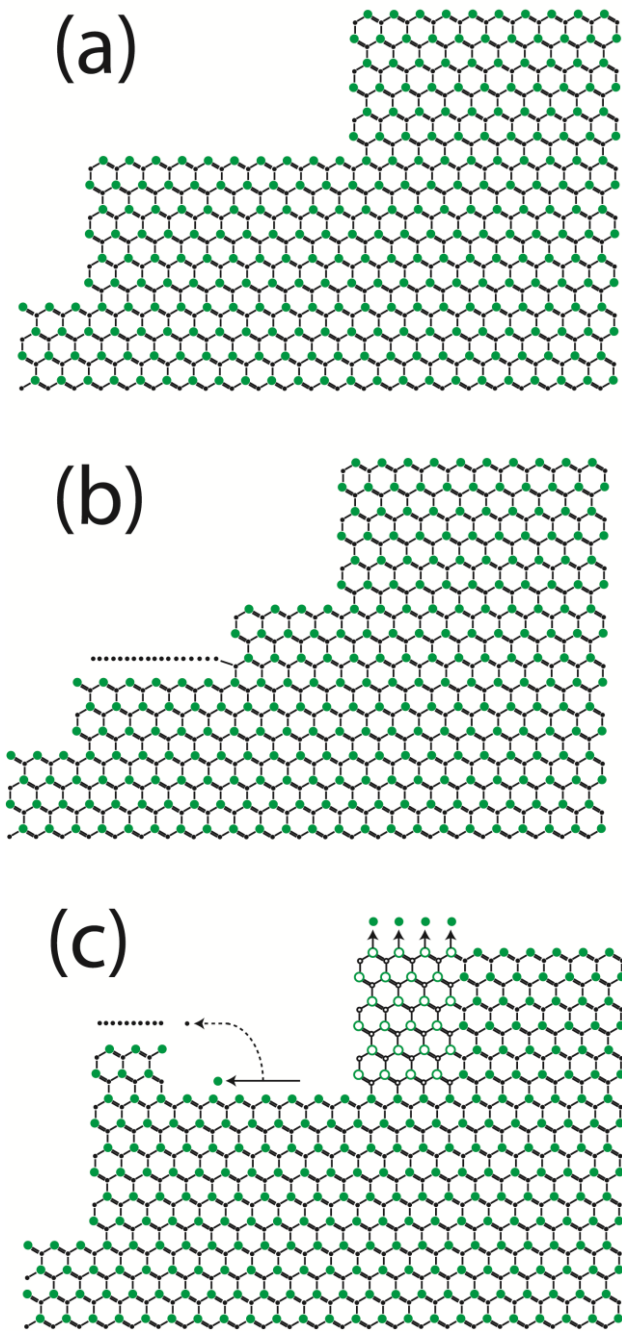


Fig 3 Schematic of graphene growth process showing bare SiC surface with bunching step (a), embedded (b) and protrusive (c) carbon layer at SiC step edge. Small and big circles indicate carbon and silicon atoms, respectively.

For annealing the 0.3 atm sample, Fig 2 (d) and (e) shows graphene morphology and shape measured near the initial state of graphene growth. These AFM results reveal that graphene is first grown at upper step edge. the AFM topography line profiles along the black line (inset) in Fig 2 (d) show the position of graphene region at the upper step edge is about 1.2 nm higher than that of SiC region on the same terrace. AFM phase (Fig 2 (e)) and SEM results Fig 2 (f)

confirm the protrusive area at upper step edge is graphene region. Although, the height of the protrusive area implies that this region should contain a buffer layer and 3 graphene layers, the thickness measurement using X-ray diffraction (XRD) reveals the presence of graphene monolayer; bilayer and trilayer on this sample are 40%, 25% and 10%, respectively [9]. Since the area in Fig 2 (d) and (e) measured around the initial state of graphene growth, the graphene thickness on the protrusive region is graphene monolayer. It implies that the protrusive area consists of SiC layers stacking at the base and a buffer layer and graphene monolayer terminating on top.

Fig 3 shows schematics of graphene growth process for 0.05 atm (Fig 3 (b)) and 0.3 atm (Fig 3 (c)) samples. A schematic in Fig 3 (a) shows the bunching steps, which appear on both samples, before graphene nucleation. In the case of 0.05 atm sample (Fig 3 (b)), the SiC substrate is first decomposed at upper step edge by Si atoms sublimation leaves behind free C atoms on the lowered area. After that those free C atoms incorporate and nucleate buffer and graphene layer, consecutively. Since the graphene position of this sample is lower than the position of SiC substrate on the same terrace, therefore there is a probability that the nucleation of bonding between C atoms at the edge of carbon layer (buffer and graphene layer) and Si or C atoms of the SiC substrate to reduce the total energy [10]. For 0.3 atm sample (Fig 3 (c)), the graphitization temperature is higher than that of 0.05 atm sample. The free C and Si atoms which were released from the SiC decomposition diffuse and incorporate at the step edge. Almost free C and Si atoms are confined at step edge due to the Schwoebel-Ehrlich barrier which increases the diffusion barrier at step edge. The free C and Si atoms prefer upward hop on top of other Si and C atoms to incorporate at the lateral. After that the Si atoms on top start sublimating allows the formation of carbon layers on top. Finally, after the annealing temperature decreases, the C and Si atoms underneath the new carbon layer form SiC layer again leads to protrusive striped graphene on SiC. Since the position of the graphene is higher than that of bare SiC terrace, there is no bonding between graphene edge and the SiC substrate. It means we can fabricate striped graphene with intact edge which is near free standing graphene on SiC.

Fig 4 shows Raman spectra of 0.05 atm (green solid line) and 0.3 atm (blue solid line) samples after the subtraction of SiC spectra. The position of G peak (near 1600 cm^{-1}) can be measured and is approximately the same for both samples. The Fig 4 inset shows the magnification of 2D peak around 2700 cm^{-1} . The 2D peaks position for the embedded graphene (0.05 atm sample) is slightly blue shifted (around 10 cm^{-1}) with respect to the protrusive sample (0.3 atm sample). The Raman peak positions of graphitic material imply 3 characteristics [11].

The first is carrier concentration. The charge doping of graphene can change the G peak position [12]-[14]. The G peak position of both samples is approximately same. It suggests that the carrier concentration of embedded and protrusive graphene is identical. It is corresponding to angle-resolved photoemission spectroscopy (ARPES) results (Fig 4 (b) and (c)) showing the same Fermi level for both samples.

The second is the graphene film strain. Mohiuddin research group found that the strain on graphene film can change the position of G and 2D peaks [15]. In our case, the G peaks of the embedded and protrusive graphene are same but only the 2D peaks of both samples are slightly different. These suggest that the both samples approximately contain the same graphene film strain although there are the bonding between graphene edge and SiC substrate in the case of embedded graphene.

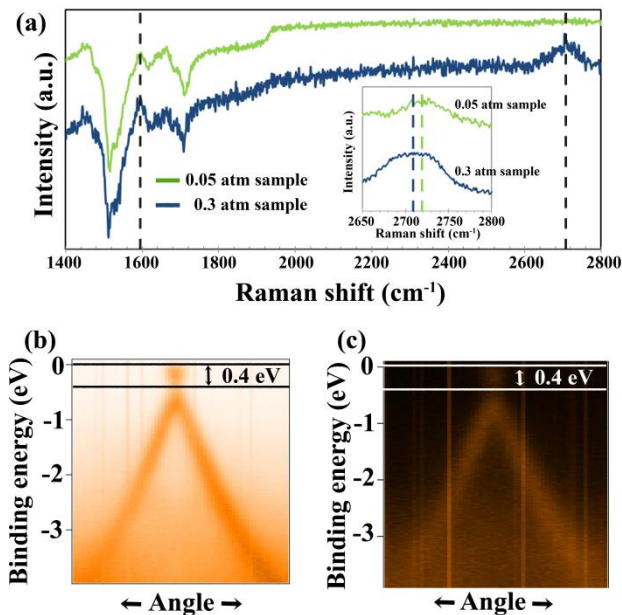


Fig 4 (a) Raman spectra after subtracted from Raman SiC spectra. Green and blue solid line indicate the samples which annealed under Ar pressure of 0.05 atm and 0.3 atm, respectively. (a) Inset Magnification of Raman spectra at the 2D peak region. (b) and (c) ARPES spectra of the 0.05 atm and 0.3 atm sample (respectively) showing Dirac cone around the K point of graphene.

The last characteristic is graphene film thickness. The graphene film thickness distribution for both samples is estimated by XRD reveals that the 0.05 atm sample (embedded graphene) consists of graphene monolayer and bilayer regions of 33% and 14%, respectively. For the 0.3 atm sample (protrusive graphene), it contains graphene monolayer of 40%, bilayer of 25% and trilayer of 10%. [9] As the number of graphene layer increase, the position of 2D peak shifts to higher wave number [16]. In this case the difference of 2D peak position of the both samples is little therefore the difference in graphene film thickness of both samples is also approximately the same. It is in good agreement with XRD results.

IV. CONCLUSION

We have grown and investigated the epitaxial embedded and protrusive striped graphene on Si-terminated 6H-SiC (0001). We found that the graphitization temperature rises from 1550 °C to 1675 °C with increment of Ar pressure from 0.05 atm to 0.3 atm. Graphene unit cell has the different angle of 30 degree from SiC unit cell. In addition, graphene prefers

to be grown and embedded at step edge for 0.05 atm sample. In the case of 0.3 atm sample, free C and Si atoms which released from the SiC decomposition diffuse to the step edge and nucleate protrusive graphene layer there. Raman peak characteristics and ARPES spectra reveal that the embedded and protrusive graphene have approximately the same carrier concentration and graphene film strain.

REFERENCES

- [1] J. Hass, W. A. de Heer, and E. H. Conrad, "The growth and morphology of epitaxial multilayer graphene," *J. Phys: Condens. Matter*, 20, 323202 (2008).
- [2] K. V. Emtsev, F. Speck, Th. Seyller, and L. Ley, "Interaction, growth, and ordering of epitaxial graphene on SiC{0001} surfaces: A comparative photoelectron spectroscopy study," *Phys. Rev. B*, 77, 155303 (2008).
- [3] A. Ismach, C. Druzgalski, S. Penwell, A. Schwartzberg, M. Zheng, A. Javey, J. Bokor, and Y. Zhang, "Direct Chemical Vapor Deposition of Graphene on Dielectric Surfaces," *Nano Lett.*, 10, 1542 (2010).
- [4] J. Tian, H. Cao, W. Wu, Q. Yu, and Y. P. Chen, "Direct Imaging of Graphene Edges: Atomic Structure and Electronic Scattering," *Nano Lett.*, 11, 3663 (2011).
- [5] L. Jiao, L. Zhang, X. Wang, G. Diankov, and H. Dai, "Narrow graphene nanoribbons from carbon nanotubes," *nature* 458 877 (2009).
- [6] F. Xia, D. B. Farmer, Y. Lin, and P. Avouris, "Graphene Field-Effect Transistors with High On/Off Current Ratio and Large Transport Band Gap at Room Temperature," *Nano Lett.*, 10, 715 (2010).
- [7] J. S. Moon, D. Curtis, M. Hu, D. Wong, C. McGuire, P. M. Campbell, G. Jernigan, J. L. Tedesco, B. VanMil, R. Myers-Ward, C. Eddy, Jr., and D. K. Gaskill, "Epitaxial-Graphene RF Field-Effect Transistors on Si-Face 6H-SiC Substrates," *IEEE electron device Lett.*, 30, 650 (2009).
- [8] A. Charrier et al., "Solid-state decomposition of silicon carbide for growing ultra-thin heteroepitaxial graphite films," *J. Appl. Phys.*, 92, 2479 (2002).
- [9] A. Ruammitree, H. Nakahara, K. Akimoto, K. Soda, and Y. Saito, "Determination of non-uniform graphene thickness on SiC (0001) by X-ray diffraction," *Appl. Surf Sci*, 282, 297 (2013).
- [10] H. Kageshima, H. Hibino, M. Nagase, Y. Sekine, and H. Yamaguchi, "Theoretical Study on Magnetoelectric and Thermoelectric Properties for Graphene Devices," *Jap. J. Appl. Phys.*, 50, 070115 (2011).
- [11] M. L. Bolen, R. Colby, E. A. Stach, and M. A. Capano, "Graphene formation on step-free 4H-SiC(0001)," *Journal of Applied Physics* 110, 074307 (2011).
- [12] Jun Yan, Yuanbo Zhang, Philip Kim, and Aron Pinczuk, "Electric Field Effect Tuning of Electron-Phonon Coupling in Graphene," *Phys. Rev. Lett.* 98,166802 (2007).
- [13] S. Pisana, M. Lazzeri, C. Casiraghi, K. S. Novoselov, A. K. Geim, A. C. Ferrari, and F. Mauri, "Breakdown of the adiabatic Born-Oppenheimer approximation in graphene" *nat. mater.*, 6, 198 (2007).

- [14] V. N. Popov, "Dynamic and charge doping effects on the phonon dispersion of graphene", Phys. Rev. b 82, 045406 (2010).
- [15] T. M. G. Mohiuddin, A. Lombardo, R. R. Nair, A. Bonetti, G. Savini, R. Jalil, N. Bonini, D. M. Basko, C. Galiotis, N. Marzari, K. S. Novoselov, A. K. Geim, and A. C. Ferrari, "Uniaxial strain in graphene by Raman spectroscopy: Gpeak splitting, Grüneisen parameters and sample orientation" Phys Rev. b 79, 205433 (2009).
- [16] D. S. Lee, C. Riedl, B. Krauss, K. V. Klitzing, U. Starke, and J. H. Smet, "Raman Spectra of Epitaxial Graphene on SiC and of Epitaxial Graphene Transferred to SiO₂" Nano Lett 8, 4320 (2008).

AUTHOR BIOGRAPHY



Akkawat Ruammaitree was born in Nakhonrachasima, Thailand. He received a B.Sc. degree in physics from Chiang Mai University, Thailand in 2007. He received his Master degree from Quantum Engineering from Nagoya University, Japan in 2011. He is recently a Ph.D. candidate in the same institution. The main research fields are the growth and characterization of epitaxial graphene in SiC.



Hitoshi Nakahara was born in Mie, Japan. He received a Bachelor's and Master degree in apply physics from Nagoya University, Japan in 1988 and 1990, respectively. He is recently a Assistant Prof. in the same institution. The main research fields are studies on inelastic electrons under reflection high-energy electron diffraction (RHEED) conditions. In addition, he also studies on self-organized nano structure formation-methods and mechanisms.



Kazuo Soda received a Ph.D. in Engineering from Nagoya University. He is recently a Prof. in Department of Quantum Engineering, Graduate School of Engineering, Nagoya University. The main research fields are Synchrotron Radiation photoelectron spectroscopy, Soft X-ray spectroscopy, Surface Science, Materials Science and Quantum beam spectroscopy.



Yahachi Saito was born in Mie, Japan. He received a Bachelor, Master degree and Ph.D. in Engineering from Nagoya University, Japan in 1975, 1977 and 1980, respectively. He is recently a Prof. in the same institution. The main research fields are first synthesis and characterization of carbon nanotubes and related material. The second is field emission from carbon nanotubes and its application to vacuum electronics. The third is crystal physics and surface science.